# Spectroscopic Analysis Study of Laser-Created Zinc Plasma

*Ahmad Z. Al-Jenaby* [iD] [✉], *Saadallah F. Hasan* [iD] [✉], *Mahmood H. Mayoof* [iD] [✉], *Abubaker S. Mohammed\** [iD] [✉]

Ministry of Education, Direction of Education in Al-Anbar, Anbar, Iraq.
*Corresponding Author.

## Abstract

Through optical emission spectroscopy, zinc (Zn) plasma produced on the basis of a laser can be investigated in the proposed study. Zinc plasma spectral emissions were studied as a function of laser energy (200, 300, 400, and 500) mJ. Record plasma emission with a 100 ns integration time. The spectral lines of zinc were determined, and the electron temperature ($T_e$) and electron density ($n_e$) were studied using Boltzmann diagrams. It is noted from the results that as the laser energies increase, the values of $T_e$ and $n_e$ rise as well, as the values range from $(1.075 - 1.467)$ eV for electron temperature, while the electron density values range $(2.939 \times 10^{18} - 3.535 \times 10^{18}) cm^{-3}$. Also, in this paper, other parameters investigated included Debye length (_D), FWHM, and plasma frequency ($f_p$).

**Keywords:** Density of electron, Electron temperature ($T_e$), Laser ND:YAG, Spectroscopic analysis, Zinc plasma.

## Introduction

Since the creation of high-potential-power lasers, numerous theoretical and empirical studies have concentrated on laser-produced plasma [1]. This plasma is created by focusing a beam of intense laser on a target's surface and then evaporating the target, resulting in very hot and extremely dense plasma. It is possible to transfer energy through a variety of mechanisms, including shock waves and radiation because of plasma density gradients [2]. Due to its uncomplicated experimental setup, the Laser Induced Breakdown Spectroscopy (LIBS) technique is a highly simple method used for element analysis. Properties of the physical and chemical environment, attributes of the medium composition and pressure of chemical mixtures, as well as characteristics of laser pulse width, spot size,

wavelength (λ), and laser irradiance, are all terms used to describe laser [3-7]. The effect of plasma on laser-to-metal energy transfer appears to be critical in a variety of applications [8]. In a plasma, density ($n_e$) and temperature ($T_e$) of electrons are the most critical properties. These characteristics are influenced by numerous empirical conditions, like wavelength, laser energy effect, and target material. To increase the measurement precision of ($T_e$) and ($n_e$) further fundamental investigations and data processing approaches are required [9,10]. The ($T_e$) and ($n_e$) are essential laser-ablated feather characteristics. These parameters have been derived on the basis of the local thermodynamic balance [11]. The collision processes that perturb the emitting ions and atoms govern the form and breadth of the

plasma-emitted spectral lines. The density of plasma may thus be derived from the line spectrum trend [12]. The plasma emission spectrum is critical for identifying and quantifying emission species in ablated material. In addition to the target material's physical and chemical qualities, laser energy, wavelength, and pulse duration all have an impact on plasma properties [13,14]. For the laser-induced Zn plasma's emission, an iterative Boltzmann approach, the electron temperature is determined, after which the alteration in the correlation coefficient and electron temperature, thus, $T_e$ may be calculated using the standard Boltzmann plot approach[15].

$$Ln\left[\frac{\lambda ij I_{ji}}{cAji g_{ji}}\right] = -\frac{1}{KT}(E_j) + \ln\left|\frac{N}{U(T)}\right| \dots\dots\dots\dots 1$$

Wherein the wavelength (in nanometers) and $I_{ji}$ are the proportional intensities (in random units) of the lines of emission among i and j levels of energy, the degeneration or empirical weight of the transition's emitting higher level I has represented as g ji., where Aij denotes the likelihood of a spontaneous change in emission of radiation from level i to level j, k is the Boltzmann constant, and $E_j$ is the level i excitation energy in eV, as well as N is represented the density of state. When a weighty particle (ion or atom) interacts with a charged particle, it causes the displacement of its two layers in a radiative transference, which causes the Stark broadening [15]. The stark line's width could be calculated by Eq. 2. [16].

## Materials and Methods

The empirical setup of the used technique is represented in Fig. 1. The pulsed laser focuses on zinc (Zn) targets using a convex-type lens, a focal length of 100 mm, at atmospheric pressures in the air and is shown in Fig. 1 with 1064 nm as the fundamental wavelength and pulse duration of 9 ns. The beam spot size was measured using an optical inspection peak scale loupe (part No. TS-1983, START International, USA) and found to be 2.2 mm. Emitted light from the plasma was picked up using an optical fiber, and optical emission spectrometer was utilized as a diagnostic instrument by evaluating surface Zn target plasma in the range of 200 mJ to 500 mJ laser energy to assess plasma properties. After focusing, Gentec-CO's MAESTRO joule meter was used to calibrate the laser energy. As the pulsed laser ablating source, a pulsed Q-switch Nd:YAG laser (Huafei Technology's (China)

$$\Delta\lambda_{FWHM} = \Delta\lambda_{observed} - \Delta\lambda_{instrument} \dots\dots\dots\dots 2$$

Where $\Delta\lambda$ is the real FWHM. Through Eq. 3, It is possible to use the spectral line widths to compute the electron density $(n_e)$ [16].

$$n_e = \left[\frac{\Delta\lambda}{2\omega_s}\right]N_r \dots\dots\dots\dots 3$$

$\omega_s$ is denotes to the theoretical line of full width Stark broadening factor, electron density $Nr \approx 1.1 \times 10^{18} cm^{-3}$. The Debye length (D) is proportional to the value of the square root of electron temperature $(T_e)$ and inversely correlated to the square root of electron density$(n_e)$. The electron plasma frequency $(\omega_{pe})$ and Debye length $(\lambda_D)$ can be calculated by Eq. 4 and 5[17].

$$\lambda_D = \left(\frac{\varepsilon_\circ KT}{n_e e^2}\right)^{1/2} \dots\dots\dots\dots 4$$

$$\omega_{pe} = \left(\frac{n_e e^2}{\varepsilon_\circ m_e}\right)^{1/2} \dots\dots\dots\dots 5$$

Where e: is the charge of the electron, mentioned above, $\varepsilon_o$ is the permittivity of free area, and $m_e$:is the mass of the electron. In this paper, we examined the spectroscopic atmospheric pressure properties created by zinc plasma in a 1064 nm Nd:YAG laser. $T_e$ and $n_e$ of the spectroscopic research using Zn plasma have been detected. The results that were obtained were examined and then contrasted with the results of the National Standards Institute and Technology (NIST).

Model HF-301 was used), Gentec Electro-Optic, Quebec City, Canada.
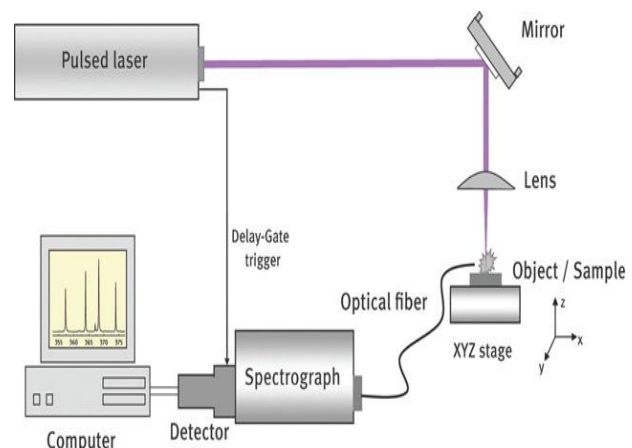


**Figure 1. Refer to the schematic experimental design [18].**

As shown in Fig. 2, the emission spectrum captured by the main channel has a strong continuous component as well as multiple neutral Zn lines.

## Results and Discussion

Fig. 2 depicts the Zn target plasma emission spectrum created by the interaction with Nd:YAG laser pulses under vacuum reaching $2 \times 10^{-2}$ mbar for Zn target plate. Spectra collected showed distinctive peaks that have been assigned based on the NIST, where each wavelength is labeled for each element as an atom or ion, and the values of A, g, $E_k$, and $E_i$ are taken.
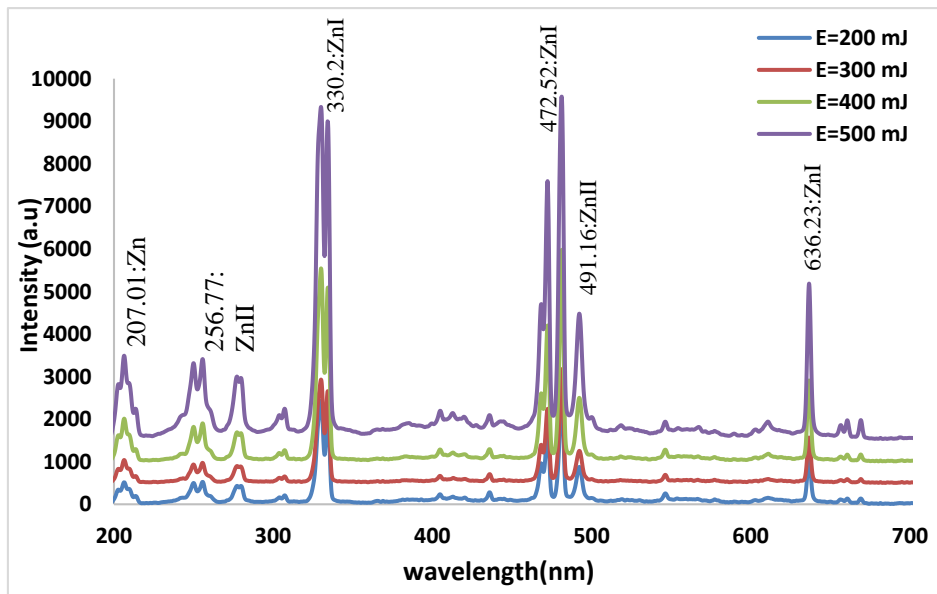


**Figure 2. Laser-induced Zn target emission spectra at different laser intensities.**

From Fig. 2, the result shows that the abstraction of laser radiation by plasma causes the emitted intensity to grow with laser energy, i.e., as the intensity increases, more of the radiation will be absorbed by the target, thus ablating a higher concentration of atoms from the target, leading to a higher concentration of atoms / ions and increase flux of light intensity emitted from the plasma. Briefly, the emitted intensity increases with laser of energy increases because of the abstraction of laser radiation by plasma, At the same time, plasma turns the laser beam transparent, thus increasing radiation and eventually increasing the spectral lines intensity, this agrees with reference [19]. In short, as the laser energy increased, intense plasmas with higher temperatures were attained; however, only a moderate increase in the density of electrons was perceived. The spectroscopic constants of Zn (II) the temperature estimation lines were taken from the NIST database [20]. Table 1 displays the calculated plasma parameters $(\lambda_D, f_p, T_e, FWHM \text{ and } n_e)$ that satisfied the standard of the plasma. The result indicates that the $f_p$ increase with laser energy increases due to the fact the plasma frequency is directly proportional with $n_e$, while $\lambda_D$ appears different value at laser energies increasing.

**Table 1. Zn plasma characteristics using diverse energy lasers.**

| Laser Energy (mJ) | $T_e$ (eV) | FWHM (nm) | $n_e*10^{18}$ (cm$^{-3}$) | $f_p$ (Hz) $*10^{13}$ | $\lambda_D$ $*10^{-6}$(cm) |
|---|---|---|---|---|---|
| 200 | 1.075 | 2.760 | 2.939 | 1.539 | 0.449 |
| 300 | 1.246 | 2.960 | 3.152 | 1.594 | 0.467 |
| 400 | 1.304 | 3.160 | 3.365 | 1.647 | 0.463 |
| 500 | 1.467 | 3.320 | 3.535 | 1.688 | 0.479 |

Where $n_e$ donates the electron density of plasma, FWHM is half, and W signifies the electron impact width parameter. The laser-induced Zn plasma has an electron density of around $3.365*10^{18}$ cm$^3$ and an electron impact width parameter corresponding to this width. The Boltzmann plot requires peaks of the same source and ionization (peak is employed in Zn II species for 481.05 nm) at Zn (pellet), as

illustrated in Fig. 3. The same figure shows the plots of ($ji$ h$c$ $Aji$ $gj$) versus $E_j$ (eV) for the various laser energy, the top energy, statistical weights, and transition probabilities can be obtained from NIST. Moreover, $T_e$ is equivalent to the opposite of the fitted line slope (the fitted line slope is equal to (-1/T). $R^2$ is a statistical indicator of the quality of a linear fit that accepts values in the range of 0-1. For all fitting lines, the linear equations and the $R^2$ are shown in Fig. 3. The higher one has an $R^2$ value closer to1 the better the fit.
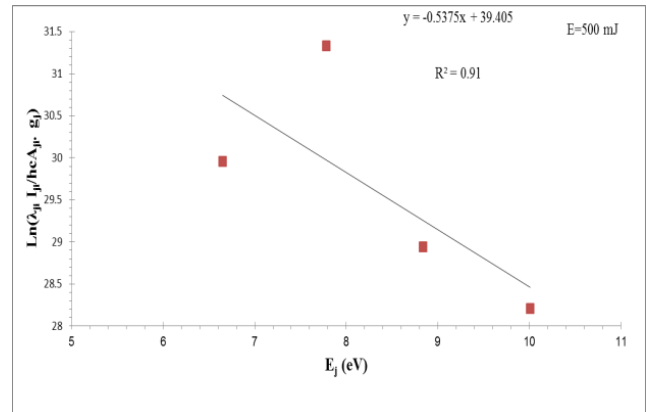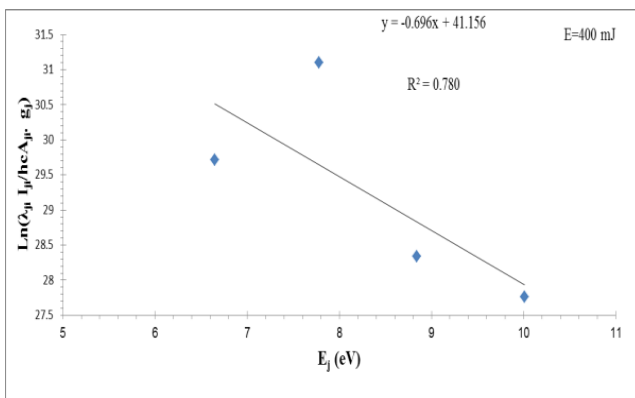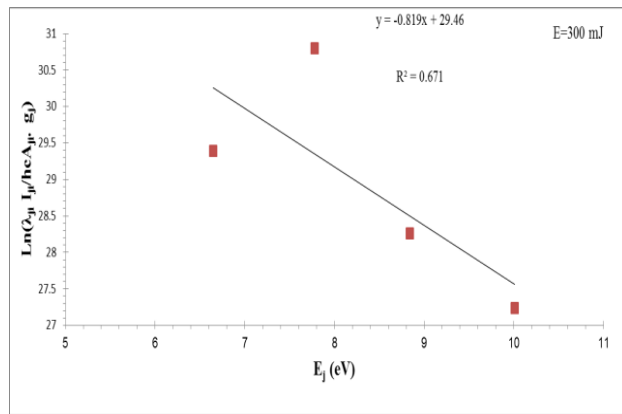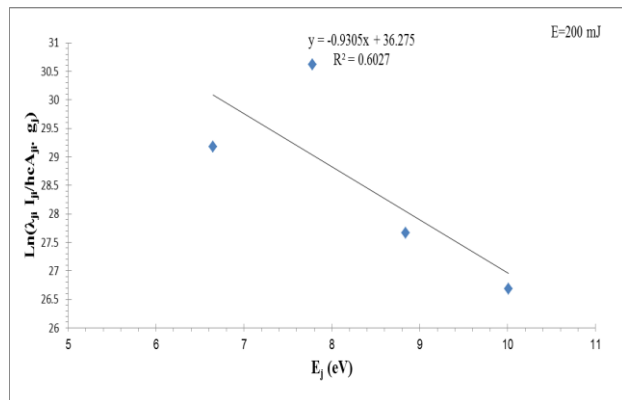




Figure 3. Boltzmann plots for Zn plasma.

The calculated electron temperatures ($T_e$) used in the Boltzmann diagram reveal that the $n_e$ and $T_e$ rise when the energy of the laser pulse increases, as illustrated in Fig. 4. Wherein the laser peak energy is increased, the laser beam is practically stable, which protects the target, and thus, the plasma will pass the laser[21].
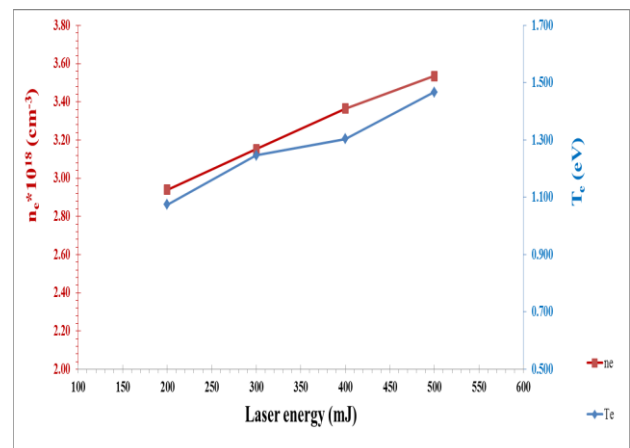


Figure 4. Shows the changes of ($n_e$) and ($T_e$) vs energy of laser for $Zn$.

## Conclusion

A Nd:YAG laser (1064 nm) was utilized for testing of plasma Zn metal. As the laser energy increases, the emitted intensity also increases, and the plasma becomes the laser beam transparent. Larger plasma (higher density) at higher temperatures was attained, and a moderate increase in the density of electrons was perceived, as all laser parameters increase with laser energy. For the transition of ionized Zn and the neutral atoms, plasma emission spectrum is given. Plasma laser emission intensities are dependent on the environmental circumstances. The intensity of the systems and nanostructures and the power of various laser spikes with high laser power are shown to increase.

## Acknowledgment

## Authors' Declaration

- Conflicts of Interest: None.
- We hereby confirm that all the Figures and Tables in the manuscript are ours. Furthermore, any Figures and images, that are not ours, have been included with the necessary permission for re-publication, which is attached to the manuscript.
- Ethical Clearance: The project was approved by the local ethical committee at Ministry of Education.
- No animal studies are present in the manuscript.
- No animal studies are present in the manuscript.
- No potentially identified images or data are present in the manuscript.

## Authors' Contribution Statement

The authors confirm their contribution to the paper as follows: study conception and design: A. Z. A.; data collection: A. Z. A., S.F. H.; analysis and interpretation of results: A. Z. A., S.F. H., M. H. M., A. S. M.; draft manuscript preparation: A. Z. A., S.F. H., M. H. M., A. S. M. All authors reviewed the results and approved the final version of the manuscript

## References

1. Mahdi SS, Aadim KA, Khalaf MA. New Spectral Range Generations from Laser-plasma Interaction. Baghdad Sci J. 2021; 18(4): 1328-1337. https://doi.org/10.21123/bsj.2021.18.4.1328.
2. Alexander P. An Introduction to Laboratory, Space,and Fusion Plasmas. 1st Edition. Springer-Verlag Berlin Heidelberg, 2010: 409 p.
3. Semerok A, Commission AE, Petite G. Femtosecond , picosecond , and nanosecond laser microablation : Laser plasma and crater investigation. Laser Part. BeamsCopyright © 2002 Cambridge University Press. 2002; 20(1): 67–72. http://dx.doi.org/10.1117/12.425562.
4. Yahya E, Bashir M A Bashir, Hussain A, Anjum I, Bahmanrokh G. Rapid fabrication of NiO / porous Si film for ultra-violate photodetector : The effect of laser energy. Microelectron Eng. 2022; 258(1): 1-7 https://doi.org/10.1016/j.mee.2022.111758.
5. Ali AH, Al-Ahmed H, Mazhir SN, Noori A S. Using Texture Analysis Image Processing Technique to Study the Effect of Microwave Plasma on the Living Tissue. Baghdad Sci J. 2018; 15(1) :87-97 doi: https://doi.org/10.21123/bsj.2018.15.1.0087.
6. Ibrahim IM, Mohammed AS, Ramizy A. Energy Band Diagram of NiO: Lu2 O3/n-Si heterojunction. Iraqi J Sci. 2018; 59(1): 287–293 https://doi.org/10.24996/ijs.2018.59.1b.6.
7. Mazhir SN, Abdullah NA, al-Ahmed HI, Harb NH, Abdalameer NK. The Effect of Gas Flow on Plasma Parameters Induced by Microwave. Baghdad Sci J. 2018; 2(2) :205-210. https://doi.org/10.21123/bsj.2018.15.2.0205
8. Shaikh NM, Rashid B, Hafeez S, Jamil Y, Baig MA. Measurement of electron density and temperature of a laser-induced zinc. J Phys D: Appl Phys. 2006; 39(1): 1384–1391. https://doi.org/10.1088/0022-3727/39/7/008
9. Kortli Y, Jridi M, Merzougui M, Atri M. Optical face detection and recognition system on low-end-low-cost Xilinx Zynq SoC. Optik. 2020; 217 (5): 164747 https://doi.org/10.1016/j.ijleo.2020.164747.
10. Abdulhadi OO, Rahmman IA, Obaid A S. Synthesis

and characterization of nickel nanoparticles formed by solution cold plasma jet. J Phys: Conf Ser. 2021: 1-12, https://doi.org/10.1088/1742-6596/2114/1/012083.

11. Shaikh NM, Hafeez S, Kalyar MA, Ali R, Baig MA. Spectroscopic characterization of laser ablation brass plasma. J Appl phys. 2008;104(10). https://doi.org/10.1063/1.3021466.

12. Harilal SS, OShay B, Tillack MS, Mathew MV. Spectroscopic characterization of laser-induced tin plasma. J Appl phys. 2005; 98(1): 1-7 https://doi.org/10.1063/1.1977200.

13. Bashir MBA, Salih EY, Rajpar AH, Bahmanrokh G, Sabri MFM. The impact of laser energy on the photoresponsive characteristics of CdO/Si visible light photodetector. J Micromech Microeng. 2022 ; 32(8): 1-8. https://doi.org/10.1088/1361-6439/ac7d93.

14. Yuan P, Wu DQ, He HP, Lin ZY. The hydroxyl species and acid sites on diatomite surface: a combined IR and Raman study. Appl Surf Sci. 2004; 227(1): 30-39 https://doi.org/10.1016/j.apsusc.2003.10.031.

15. Abdaalameer N Kh, Mazhir SN, Aadim KA. Diagnostics of zinc selenite plasma produced by FHG of a Q-switchedND: YAGlaser. Chalcogenide Lett. 2021; 18(7): 405-411 https://doi.org/10.1134/S0030400X15070127.

16. Mohamed F, Tawfik W, Omar MM. Investigation on the effects of laser parameters on the plasma profile of copper using picosecond laser induced plasma spectroscopy. Opt Quantum Electr. 2020; 52 : 1-16 https://doi.org/10.1007/s11082-020-02381-x .

17. Mohammed RS, Aadim KA, Ahmed KA. Spectroscopy diagnostic of laser intensity effect on Zn plasma parameters generated by Nd: YAG laser. Iraqi J Sci. 2022; 63(9): 3711-3718 https://doi.org/10.24996/ijs.2022.63.9.5.

18. Khidhir AH, Mohammed AH. Using Laser-induced breakdown spectroscopy system to determine the fertility of middle Iraqi soil. Iraqi J Sci. 2018. 59(4): 2012-2019 https://doi.org/10.24996/ijs.2018.59.4B.7.

19. Pace, DMD, Graciela B, Cristian ADA. Characterization of laser–induced plasmas by atomic emission spectroscopy. J Phys Conf Ser. 2011; 274(1) : 1-21 https://doi.org/10.1088/1742-6596/274/1/012076.

20. Hutchinson IH. Principles of plasma diagnostics. 2nd Ed . Plasma Phyics and Controlled Fusion. 2012; 44(12): 2603-2613 https://doi.org/10.1088/0741-3335/44/12/701.

21. Qindeel R, Dimitrijević MS, Shaikh NM, Bidin N, Daud YM. Spectroscopic estimation of electron temperature and density of zinc plasma open air induced by Nd: YAG laser. Eur Phys J-Appl Phys. 2010; 50(3): 30701-7 https://doi.org/10.1051/epjap/2010047.

## دراسة التحليل الطيفي لبلازما الزنك المكونة بالليزر

احمد زيدان الجنابي، سعدالله فياض حسن، محمود هاشم معيوف ، ابوبكر صبار محمد

وزارة التربية والتعليم، مديرية التربية والتعليم في محافظة الانبار، الانبار، العراق.

الخلاصة

من خلال التحليل الطيفي للانبعاثات الضوئية ، يمكن فحص بلازما الخارصين (Zn) المنتجة على أساس الليزر في هذه الدراسة المقترحة. حيث تمت دراسة الانبعاثات الطيفية لبلازما الخارصين كدالة لتغيير طاقات الليزر (200, 300, 400, 500) ملي جول. سجلت انبعاث البلازما مع وقت تكامل 100 نانو ثانية. تم تحديد الخطوط الطيفية لمادة الخارصين ودراسة درجة حرارة الالكترون وكثافة الالكترون عن طريق مخططات بولتزمان. يلاحظ من النتائج أنه مع زيادة طاقات الليزر , ترتفع قيم كلا من درجة حرارة الالكترون وكثافة الالكترون, حيث تتراوح قيم درجة الحرارة (1.075 -1.467 الكترون فولت بينما تتراوح قيم كثافة الالكترون بحدود (2.939×$(10)^{18}$-3.535 × $(10)^{18}$ ). سم3, أيضا في هذا البحث تمت دراسة معاملات أخرى مثل طول ديباي , عرض منتصف القمة و تردد البلازما.

الكلمات المفتاحية: كثافة الالكترون, درجة حرارة الالكترون, ليزر الندميوم- ياك, التحليل الطيفي , بلازما الخارصين.